

39. INTERSTITIAL-WATER CHEMISTRY: ABYSSAL SOUTH ATLANTIC AND EAST GEORGIA BASINS, ISLAS ORCADAS AND METEOR RISES¹

P. N. Froelich,² R. A. Mortlock,² M. Mefferd,³ and J. Powers³

ABSTRACT

Pore-water samples were recovered at five sites from ODP Leg 114 in the subantarctic South Atlantic Ocean and analyzed for pH, alkalinity, chloride, sulfate, fluoride, silica, magnesium, calcium, strontium, potassium, lithium, and barium. At sites in the East Georgia Basin and on the Islas Orcadas Rise, Ca increases and Mg decreases linearly downhole with a $\Delta\text{Mg}/\Delta\text{Ca}$ ratio reflecting conservative diffusive exchange and basalt basement reactions. At sites on the west flank of the Mid-Atlantic Ridge and on the Meteor Rise, Ca gradients are nonlinear, and nonconservative $\Delta\text{Mg}/\Delta\text{Ca}$ ratios reflect alteration reactions of abundant silicic volcanic ash in the sediment. K decreases linearly downhole at all sites, reflecting uptake by basement and the absence of significant sediment-hosted reactions. SO_4 decreases and alkalinity increases downhole are due to a slight sulfate reduction at all sites except at Site 701. Sr increases downhole at all sites except Site 701, with $\Delta\text{Sr}/\Delta\text{Ca}$ ratios reflecting diffusive exchange with basement. At Site 704 on the Meteor Rise, there is intense Sr production during carbonate recrystallization in the upper 200 mbsf. Below 200 mbsf at Site 704, the ion concentration product of SrSO_4 is constant, suggesting Sr control by celestite solubility. Li and F concentrations display complex behavior related to sedimentary reactions, probably calcite recrystallization (Li uptake and F release).

INTRODUCTION

Ocean Drilling Program (ODP) Leg 114 consisted of a longitudinal transect across 50°S in the subantarctic South Atlantic between latitudes of 31°W and 8°E. Sites were occupied in the East Georgia Basin, the abyssal South Atlantic Ocean (western flank of the Mid-Atlantic Ridge), and atop the Islas Orcadas and Meteor rises (Table 1). The major objectives of this leg were to recover continuous Neogene and Paleogene sections to reconstruct the paleoceanography of the South Atlantic during the initiation of Antarctic glaciation and to monitor the development and northward migration of the global circumpolar Antarctic circulation and deep- and bottom-water flow paths as oceanic gateways opened among Africa, South America, and Antarctica. Recovered sections range in age from Late Cretaceous through Quaternary with a lithology encompassing siliceous and calcareous oozes, cherts, limestones (no dolomite), volcanic ashes, zeolites, cherts, and basement (Table 1). As such, these sections represent a wide variety of lithology within which to investigate reactions controlling the behavior of pore-water constituents. Our particular interest in this leg arose from the possibility of recovering complete high-latitude Neogene bio-siliceous sections in which to study late Oligocene through Quaternary biogenic opal production, dissolution, preservation, and diagenesis and to reconstruct a high-resolution record of $(\text{Ge}/\text{Si})_{\text{opal}}$ variations in sediments that had been well studied geochemically (Shemesh et al., 1989; Froelich et al., 1989). The results of this latter work are not complete at this writing and will be presented with a discussion of silica diagenesis elsewhere.

METHODS

All pore waters were expressed with stainless-steel squeezers in hydraulic presses from 5- or 10-cm whole-round samples cut from the cores immediately after retrieval (Manheim and Sayles, 1974). For Sites 699, 700, and 701, pore fluids were expressed at ambient temperatures directly into pre-cleaned polyethylene syringes, and then post-filtered through 0.4- μm membrane filters into pre-cleaned polyethylene vials (for shipboard determinations) and bottles (for transport to the laboratory). For Sites 702 and 704, the squeezers were maintained at bottom-water temperatures in a refrigerator (2°–4°C) prior to loading sediment in an attempt to eliminate temperature-of-extraction artifacts for F, Li, Ba, and Si. For these two sites, pore waters were expressed into a syringe through a 0.4- μm membrane filter held in a syringe filter holder that was inserted directly into the squeezer port. The contents of the syringes were again post-filtered into vials and bottles. The temperature of the effluent fluid increased less than 2°C during pore-water extraction, indicating that the squeezers have sufficient thermal inertia to maintain the initial temperature over the 10–20 min required for squeezing the high-porosity, poorly consolidated sediments of these holes.

Values of pH, alkalinity, salinity, chloride, calcium, magnesium, and sulfate were determined aboard ship using standard ODP methods (Table 2). The pH, alkalinity, and salinity were measured immediately after pore-water extraction, and chloride, calcium, magnesium, and sulfate were generally run within 24 hr of collection. Silica was determined aboard ship within four days with a technique modified from Mortlock and Froelich (1989). Fluoride was determined immediately aboard ship by fluoride specific-ion combination electrode using the method of Froelich et al. (1983). The methods of analyses and calibrations for all shipboard determinations are described in detail in the "Explanatory Notes" (Shipboard Scientific Party, 1988).

Potassium, strontium, lithium, and barium were determined in the shorebased laboratory at Lamont-Doherty Geological Observatory from splits (unacidified) of the same samples ana-

¹ Ciesielski, P. F., Kristoffersen, Y., et al., 1991. *Proc. ODP, Sci. Results, 114*: College Station, TX (Ocean Drilling Program).

² Lamont-Doherty Geological Observatory, Columbia University, Palisades, NY 10964.

³ Ocean Drilling Program, Texas A&M University, 1000 Discovery Drive, College Station, TX 77845-9547.

Table 1. Pore-water sampling sites, Leg 114.

Site	Location	Age	Lithology	Water depth (m)	Temperature ^a (°C)
699	East Georgia Basin 51°32.537'S, 30°40.619'W	early Eocene to early Miocene	Diatomaceous clay, siliceous nannofossil ooze-chalk-micrite, with zeolitic clay near basement	3706	22
700	East Georgia Basin 51°31.992'S, 30°16.697'W	early Campanian to late middle Eocene	Nannofossil ooze-chalk-micrite-limestone	3601	22
701	West flank of Mid-Atlantic Ridge 51°59.07'S, 23°12.73'W	early Eocene to Quaternary	Diatomaceous ooze, with ash, nannofossil ooze-chalk, basal zeolites overlying mid-ocean ridge basalt	4627	22
702	Islas Orcadas Rise 50°56.786'S, 26°22.117'W	late Paleocene to late Miocene	Nannofossil-diatom ooze-chalk, trace ash + chert stringers, basal silicified limestone + zeolites	3083	4
704	Southern Meteor Rise 46°52.757'S, 07°25.250'E	middle Oligocene to Quaternary	Diatom-calcareous ooze, micritic nannofossil chalk, with dispersed volcanic ash	2532	4

^a At which pore waters were extracted (see text).

lyzed aboard ship (Table 2). These samples were maintained at 4°C in a humidified core-storage locker for longer than 1 yr before being analyzed. Potassium was determined by flame emission with a Perkin Elmer 5000 Atomic Absorption Spectrometer. Samples and standards were diluted by a factor of 200 with a 20-mM NaCl solution. Strontium and lithium were determined by flame atomic absorption spectrometry. For strontium, samples and standards were diluted by a factor of 20 with a 0.1% lanthanum solution and determinations were by standard additions of Sr. For lithium, samples were diluted 1:1 with distilled-deionized water (DDW), and standards (in a DDW matrix) were diluted 1:1 with a 500-mM NaCl solution. Barium was determined by graphite-furnace atomic absorption spectrometry using Zeeman background correction. Samples and standards were diluted to the range of 0–250-nM Ba with DDW. Strontium isotopes and inorganic germanium are also being determined on these samples, the results of which will be reported elsewhere.

RESULTS

The pore-water data from all sites are presented in Table 3 and plotted vs. sub-bottom depth in Figure 1. The water depth, lithology, and age of each site are summarized in Table 1. In general, the pore-water profiles at these sites can be related to several processes (Gieskes, 1981): (1) downward diffusion of late Pleistocene oceanic salinity variations imparted by the waxing and waning of continental glacial ice (salinity and chloride); (2) diffusion through the sediment column between the overlying water column and basement reactions involving low-temperature basalt-seawater interactions (Ca, Mg, K, Sr, and Li); (3) sedimentary silicic volcanic ash alteration reactions (Ca, Mg, and Li); (4) sedimentary calcite recrystallization reactions (Sr, F, and Li); and (5) silica diagenesis (Si). In the following discussions, we will briefly consider the effects of the first four of these processes on the pore-water profiles at Leg 114 sites.

DISCUSSION

Salinity Variations

Downhole salinity and chloride variations at these sites are likely caused by variations in bottom-water salinity during the

Table 2. Pore-water analytical methods.

Analyte	Method	Reference
pH	Glass electrode	Gieskes and Peretsman (1986)
Alkalinity	Potentiometric Gran titration	Gieskes and Peretsman (1986)
Salinity	Refractometer	
Mg	Colorimetric titration	Gieskes and Peretsman (1986)
Ca	Colorimetric titration	Gieskes and Peretsman (1986)
Cl	Colorimetric titration	Gieskes and Peretsman (1986)
SO ₄	Ion chromatography	Gieskes and Peretsman (1986)
F	Specific ion electrode	Froelich et al. (1983)
Si	Molybdate-blue spectrophotometry	Mortlock and Froelich (1989)
Sr	Flame atomic absorption spectrometry	Gieskes (1974)
K	Flame emission	Gieskes (1974)
Li	Flame atomic absorption spectrometry	von Damm (1983)
Ba	Graphite-furnace atomic absorption spectrometry with Zeeman correction	Bishop (1990)

late Pleistocene (McDuff, 1985). Changes in the salinity of the overlying water impart diffusion gradients downward into the sediment column, the amplitude of which is damped with increasing depth. Thus the "ages" of such variations increase exponentially with increasing sub-bottom depth and are not linked to stratigraphic age. These changes have been previously linked to whole-ocean changes in salinity caused by the waxing and waning of the continental ice sheets. While this is undoubtedly the major global cause behind these observations, we suggest here that local water mass variations may also be involved. Paleoceanographic inferences can thus be drawn from differences in the chloride profiles at our sites. Sites 699 and 702 (both in the western Atlantic) and 704 (in the eastern Atlantic) display chloride profiles with near-surface minima (low Holocene-ocean salinities) and sub-bottom maxima at 20 to 50 m below seafloor (mbsf) (higher glacial-ocean salinities), below which chloride concentrations slowly decrease (pre-Pleistocene low-salinity ocean) (Fig. 2). The shapes of these profiles are fairly typical of "normal" pelagic sites (McDuff, 1985). These three sites are at mid-water depths

(2500–3700 m) under the influence today of Circum-Polar Deep Water (CPDW), with Site 704 being more influenced by high-salinity North Atlantic Deep Water (NADW). The time scale for diffusion to sub-bottom depths of 20 to 50 mbsf is 100,000 to 700,000 yr, suggesting that average deep-water salinities were higher at these three sites over this period of intense late Pleistocene glaciation. The magnitude of the increase is both greater and of longer duration than at Site 704, suggesting that the upper deep water in the eastern South Atlantic Ocean was more influenced by NADW than in the western basin. In addition, the salinities of Sites 699, 702, and 704 converge on the same values below 150 mbsf. The time scale for diffusion to 150 mbsf is about 6,000,000 yr, suggesting that these three sites experienced the same salinities prior to the late Miocene.

In contrast, Site 701 is in a water depth of 4600 m, positioned within the main pathway of northward Antarctic Bottom Water (AABW) flow from the Weddell Sea into the Argentine Basin. This bottom-water site is remarkable in two important respects: (1) the absence of significant salinity (chloride) variations downhole and (2) salinities (chlorides) that are always lower than at the shallower sites for depths greater than 10 mbsf. Apparently, bottom-water salinities over Site 701 have not varied significantly over the last several million years. This suggests that AABW flow northward has been continuous over the last several million years and has not varied greatly in salinity.

Basalt Basement Reactions vs. Silicic Volcanic Ash Alteration

Concentrations of calcium increase and those of magnesium and potassium decrease downhole at all sites. Potassium decreases are fairly linear at all sites, suggesting the absence of significant sedimentary reactions and control by low-temperature K uptake into basement.

At Sites 699, 700, and 702, the downhole gradients in Ca and Mg are linear with depth and reflect diffusional gradients between the overlying seawater and basalt-seawater reactions occurring in basement (McDuff, 1981; Gieskes, 1983; Gieskes et al., 1984). The calcium vs. magnesium relationship at these three sites is linear with a $\Delta\text{Mg}/\Delta\text{Ca}$ slope of -0.5 (Fig. 3B), a typical "conservative" profile diagnostic of basalt basement reactions (Baker, 1986). Thus, the pore-water data are consistent with the interpretation that basements of the East Georgia Basin and the Islas Orcadas Rise are composed of basalt and with the observed absence of either dolomite or volcanic ash within the sediment at these three sites.

Sites 701 and 704, on the other hand, while displaying linear downward K gradients, show nonconservative Ca and Mg gradients resulting from alteration reactions of silicic volcanic ash throughout the upper part of the section (Gieskes and Lawrence, 1981; Gieskes, 1983; Baker, 1986). Sedimentary ash reactions apparently dominate the Ca and Mg profiles so that diffusive exchange between seawater and the underlying basaltic basement reactions do not control the Mg/Ca ratio. The vertical profiles of Ca and Mg at Sites 701 and 704 are thus nonlinear, and the Ca vs. Mg trend is also nonlinear but approaches a slope of -2.0 (Fig. 3B), which is characteristic of reactions with silicic minerals (Baker, 1986). This is again consistent with the observation of abundant ash horizons at Site 701 and dispersed ash within the upper 50 m at Site 704. Sites 701 and 704 are farther east than the other sites of Leg 114 and presumably received ash falls from explosive volcanic eruptions in the Scotia Arc, which is 510 km southwest and upwind of Site 701.

Pore-water lithium profiles at Sites 699, 700, and 702 display approximately linear downward-increasing gradients that parallel the calcium gradients, suggesting diffusive exchange with basement reactions (Fig. 1). The profile at Site 701 shows a maximum at about 300 mbsf, with apparent production of Li throughout the sediment column between about 300 and 450 mbsf. This behavior may be linked to the alteration of abundant silicic volcanic ash. At Site 704, on the other hand, the lithium profile displays a dramatic minimum at 200–300 mbsf, requiring Li consumption reactions within this interval. A plot of Li vs. K for these sites (Fig. 3C) demonstrates the lack of any simple relationship, although it is clear that the sites in the East Georgia Basin (Sites 699 and 700) and on the outer flank of the Mid-Atlantic Ridge (Site 701) display higher Li/K gradients than the two sites atop the conjugate Islas Orcadas (Site 702) and Meteor (Site 704) rises. A plot of Li/Ca (normalized for basement exchange) vs. fluoride (Fig. 3D) suggests that fluoride and lithium behave inversely during sediment diagenesis, a point that will be discussed further in the following text.

Sedimentary Calcite Recrystallization

The most sensitive indicator of calcite dissolution is strontium. In the Leg 114 sites, Sr displays three distinct styles of behavior: (1) unreactive (Site 701), (2) diffusive exchange with basement (Sites 699, 700, and 702), and (3) carbonate recrystallization (Site 704). Site 701, the deepest of our sites, displays Sr concentrations only slightly elevated above bottom-water concentrations ($90 \mu\text{M}$). Thus we infer that there are no contemporaneous calcite recrystallization reactions occurring in the sediment column at Site 701, where the sediments are devoid of carbonate, and that Sr release from basement reactions is small. In contrast, at Sites 699, 700, and 702, Sr increases rapidly and linearly downhole, with a constant $\Delta\text{Sr}/\Delta\text{Ca}$ slope of about 36×10^{-3} (Fig. 3A). We infer that this behavior reflects diffusive exchange with reactions releasing Sr from below the recovered interval, perhaps basal carbonate recrystallization reactions.

Site 704 displays dramatically different behavior. Here Sr increases rapidly in the upper 200 m to over $1000 \mu\text{M}$, and then plateaus with concentrations increasing more slowly in the bottom 500 m. The $\Delta\text{Sr}/\Delta\text{Ca}$ slope in the upper part of the section is about 220×10^{-3} , indicative of Sr exclusion from biogenic carbonates (possibly including aragonite) upon recrystallization to calcite. At high concentrations, Sr may be controlled by celestite (SrSO_4) solubility (Baker, 1986). A plot of Sr vs. SO_4 (Fig. 4A) demonstrates an indirect relationship between Sr and SO_4 at all sites except Site 701, reflecting downward-decreasing sulfate and -increasing strontium suggestive of celestite solubility control. However, a plot of the ion concentration product of celestite (ICP) vs. sub-bottom depth for all sites (Fig. 4B) demonstrates that near-constant values of the ICP are reached only below 200 mbsf at Site 704 and near the bottoms of Sites 699 and 702. The higher apparent solubility product for celestite at Site 704 on the Meteor Rise (ICP = 21×10^{-3}) compared to the Lord Howe Rise sites (ICP = 15×10^{-3} ; Baker, 1986) may be related to the greater water depth for the Meteor Rise site and thus an increase in the solubility product at greater pressures (Baker and Bloomer, 1988). No celestite nodules were observed at Site 704.

Fluoride is released during calcite dissolution and recrystallization reactions. At Site 704, fluoride increases dramatically downhole to a maximum concentration about four times that of seawater by 300 mbsf. Biogenic carbonates

Table 3. Leg 114 pore-water data.

Core, section, interval (cm)	Depth (mbsf)	pH	Alkalinity (mM)	Salinity (‰)	Mg (mM)	Ca (mM)	Cl (mM)	SO ₄ (mM)	F (μM)	Si (μM)	Sr (μM)	K (mM)	Li (μM)	Ba (nM)
114-699A-														
1H-4, 145-150	5.9	7.73	3.09	34.2	51.48	10.88	554.1	28.30	62.2	822	127	10.66	26.0	693
3H-3, 145-150	22.5	7.46	3.45	35.4	51.24	12.49	569.9	27.90	41.1	730	140	10.31	26.0	593
6H-5, 145-150	54.0	7.83	4.08	35.0	48.89	14.60	568.9	26.80	41.4	872	197	10.40	42.8	640
9H-4, 145-150	81.0	7.78	4.50	35.0	47.85	16.12	565.9	26.30	41.9	984	230	10.79	57.8	495
12H-4, 145-150	109.5	7.76	4.51	35.0	47.47	18.04	566.9	25.10	36.0	950	257	10.22	73.6	392
15H-3, 145-150	136.5	7.46	4.79	35.0	45.80	19.63	560.0	25.10	30.9	997	303	10.00	83.5	505
18H-4, 145-150	166.5	7.22	4.54	34.8	44.73	20.85	561.0	24.80	28.5	1152	341	9.39	96.6	483
21H-4, 140-150	195.0	7.24	4.71	34.8	43.37	22.85	565.9	24.30	25.9	1090	383	9.39	108.0	451
24X-2, 140-150	217.5	8.14	4.94	34.8	43.74	22.84	567.9	24.40	22.2	1073	408	8.42	110.0	688
30X-3, 140-150	273.0	7.25	5.60	35.0	40.59	26.67	568.9	23.90	19.0	1094	479	8.33	135.0	446
33X-5, 140-150	304.5	7.23	5.23	35.0	40.75	26.75	570.0	23.60	19.4	1032	490	8.38	135.0	550
36X-5, 140-150	333.0	7.25	4.98	34.8	38.81	28.85	569.9	23.60	17.5	1146	488	7.02	145.0	2058
39X-1, 140-150	355.5	(7.85)	(4.79)	(34.0)	(41.18)	(33.58)	(536.2)	(21.00)	(16.3)	(655)				
42X-5, 140-150	390.0			(33.7)	(39.51)	(36.27)	(539.2)	(20.30)	(19.3)	(595)	(711)	(4.65)	(194.0)	(1320)
45X-5, 140-150	418.5			33.8	37.02	35.36	559.0	22.10	26.1	508	915			
48X-4, 140-150	445.5	7.19	3.56				555.0	25.20	34.5	408	556	7.31	115.0	2736
48X-4, 140-150	445.5	(7.43)	(3.71)	(33.8)			(551.1)		(33.8)	(484)	(563)	(7.24)	(128.0)	(1127)
54X-1, 140-150	498.0			32.3	33.60	38.62	531.2	19.40	30.2	577	1018			
114B-700B-														
3R-1, 145-150	27.8	7.76	3.70	34.6	51.57	12.02	553.2	26.72	76.1	761	150	10.88	35.7	1895
6R-5, 145-150	62.3	7.55	4.01	34.8	48.91	14.52	548.3	25.32	60.2	418	218	10.44	42.0	759
9R-5, 145-150	90.8	7.20	4.06	35.2	48.07	17.02	555.1	24.74	58.3	379	331	10.44	49.5	530
13R-4, 140-150	127.3	7.55	3.95	35.0	46.28	19.37	556.1	25.16	58.7	605	369	9.39	52.0	1642
16R-5, 140-150	157.3	7.35	5.12	35.2	44.50	22.96	561.9	23.98	60.6	465	467	8.90	60.1	1014
20R-2, 140-150	190.8	7.63	4.35	35.0	43.50	23.49	555.1	24.04	61.9	569	501	9.65	62.7	1146
26R-2, 140-150	240.9	7.45	4.26	35.0	39.98	28.51	549.3	22.82	54.2	1131	628	7.41	75.2	2766
114-701A-														
1H-4, 145-150	5.9	7.69	4.21	34.8	52.67	10.99	558.0	27.30	61.6	811	97	9.83	24.4	644
3H-4, 145-150	23.7	7.73	5.00	35.0	52.32	11.35	557.0	26.80	43.6	950	98	10.09	24.4	1029
6H-5, 145-150	53.7	7.69	5.66	35.0	50.59	12.13	558.0	25.40	33.9	861	119	9.83	30.1	544
114-701B-														
1H-5, 145-150	77.4	7.62	6.03	34.8	49.51	12.13	554.0	24.50	30.9	969	119	10.53	35.7	699
4H-5, 145-150	105.9	7.59	6.19	34.6	47.95	12.87	555.0	24.40	27.7	979	127	10.09	42.6	536
7H-4, 145-150	132.9	7.58	6.33	34.2	46.50	13.29	553.0	24.10	25.6	1044	122	10.00	47.0	585
9H-5, 46-50	150.0	7.72	5.95	34.5	46.62	13.49	558.0	24.50	30.5	1320	129	10.62	52.0	1058
13H-3, 140-150	188.4	7.51	6.60	34.3	45.95	14.02	557.0	23.00	28.2	1080	136	9.65	59.5	489
114-701C-														
23H-4, 140-150	155.7	7.74	6.47	34.6	46.62	13.67	553.0	24.09	24.2	1171	133	9.65	52.6	613
27H-2, 140-150	211.7	7.82	6.67	34.2	45.95	14.18	551.0	23.65	25.1	1063	117	10.18	61.4	46
27H-2, 140-150	246.7	7.77	6.27	34.0	45.09	14.33	549.0	21.14	27.7	1184	137	9.08	65.8	720
31X-2, 140-150	284.7	7.68	6.05	34.5	45.32	14.65	550.0	23.45	27.7	962	137	8.99	65.8	492
34X-4, 140-150	316.2	7.89	6.28	34.4	43.64	15.03	550.0	23.90	26.2	1028	128	9.34	67.0	496
37X-3, 140-150	343.2	7.65	6.33	34.0	43.71	15.26	546.0	24.17	27.7	1083	130	9.34	65.8	490
42X-1, 140-150	387.7	7.61	6.11	33.8	49.53	16.27	543.0	23.40	29.8	1192				
45X-4, 140-150	420.7	7.76	5.34	34.1	46.80	15.93	544.0	23.13	28.3	1167	105	8.55	58.9	741
49X-4, 140-150	458.7	7.74	4.61	34.5	47.56	15.01	550.0	24.93	37.7	633	126	8.64	52.0	967

contain about 200 ppm fluoride, which is incorporated from seawater during rapid growth of calcitic tests (Froelich et al., 1983). Upon near-equilibrium dissolution and reprecipitation, inorganic calcite excludes F, partitioning it into the interstitial solution, similar to Sr. Thus, F gradients are sensitive indicators of contemporaneous carbonate recrystallization reactions in calcareous sediments. However, the F profile at Site 704 also requires that F be consumed by some unknown sedimentary reaction at 550 mbsf. The inverse behavior of F and Li at Site 704 suggests that these reactions may involve both constituents (Fig. 3D). Similar F consumption reactions may be occurring in other sites, where the shapes of the F profiles suggest uptake reactions in the sediment column. Whether this is an artifact of the pore-water extraction process (Froelich et al., 1983), or perhaps disseminated precipitation of trace carbonate-fluorapatite (francolite), is unknown.

CONCLUSIONS

Pore-water profiles in the Leg 114 holes can be used to infer chemical reactions occurring in the sediment column and in

basement below the recovered section. Characteristic calcium and magnesium gradients confirm that basement under the East Georgia Basin and Islas Orcadas Rise (and, by analogy, the conjugate Meteor Rise) are basaltic in composition. These gradients on the Meteor Rise and the western flank of the Mid-Atlantic Ridge are obscured by sediment-hosted silicic volcanic ash alteration reactions. Carbonate dissolution and recrystallization reactions are inferred from fluoride and strontium profiles to dominate the biogenic oozes atop the Meteor Rise, where strontium concentrations approach equilibrium with celestite within 200 mbsf. Lithium and fluoride are involved in both sedimentary production and consumption reactions linked to carbonate diagenesis and other as yet unidentified processes. Salinity (chloride) gradients in the upper 200 m of these sites suggest that while sites at intermediate water depths on the Islas Orcadas and Meteor rises and in the East Georgia Basin underwent higher bottom-water salinities during the late Pleistocene, the deepest site in the main channel of AABW flow northward from the Southern Ocean into the Atlantic has experienced no salinity changes in the last few million years.

Table 3 (continued).

Core, section, interval (cm)	Depth (mbsf)	pH	Alkalinity (mM)	Salinity (‰)	Mg (mM)	Ca (mM)	Cl (mM)	SO ₄ (mM)	F (μM)	Si (μM)	Sr (μM)	K (mM)	Li (μM)	Ba (nM)
114-702A-														
1H-2, 145-150	2.9	7.70	2.92	34.2	53.29	10.88	552.0	29.14	67.0	793	111	9.52	25.1	896
3H-5, 145-150	21.5	7.65	2.93	35.0	53.40	11.57	561.0	28.28	65.0	819	125	9.56	28.2	398
114-702B-														
1H-3, 145-150	4.4	7.57	3.00	34.7	53.59	10.90	556.0	28.63	67.5	802	99	10.02	25.7	463
3H-5, 145-150	23.2	7.58	2.96	34.5	53.15	11.66	564.0	27.79	70.3	762	137	10.22	25.1	414
6X-1, 145-150	45.7	7.62	3.02	34.8	52.01	13.12	563.0	27.30	68.1	787	176	9.30	25.7	351
9X-4, 145-150	78.7	7.54	2.85	34.4	50.91	14.61	560.0	27.10	71.7	749	222	9.08	25.7	465
12X-5, 145-150	108.7	7.61	2.92	34.5	48.57	16.95	559.0	26.38	68.9	787	332	10.00	28.8	596
15X-5, 145-150	137.2	7.57	2.74	34.6	47.30	18.94	564.0	25.91	70.3	730	367	9.04	27.6	810
18X-5, 145-150	165.7	7.38	2.94	34.6	45.63	21.00	566.0	25.36	76.7	798	433	8.29	26.3	823
21X-2, 145-150	189.7	7.38	2.82	34.9	45.13	22.23	564.0	25.46	81.7	560	468	8.11	26.3	1033
24X-2, 145-150	218.2	7.47	2.68	35.0	43.34	24.42	564.0	25.61	92.8	500	540	7.85	26.9	675
30X-1, 145-150	273.7	7.42	2.47	35.2	41.15	28.68	565.0	25.15	99.7	619	701	8.03		1740
114-704A-														
1H-4, 145-150	5.9	7.75	3.14	34.5	54.82	10.63	567.0	28.42	70.2	840	104	9.65	25.1	384
3H-5, 145-150	24.1	7.70	3.46	34.9	56.15	11.38	582.0	30.02	72.2	1009	124	10.44	22.6	283
6H-3, 145-150	49.6	7.64	3.90	35.2	55.95	11.58	583.0	29.94	62.8		131	10.18	19.4	294
9H-4, 145-150	79.6	7.66	4.05	34.9	55.19	11.46	582.0	29.31	64.1		155	9.69	16.3	257
12H-5, 145-150	109.6	7.59	3.99	35.0	52.90	11.35	576.0	28.05	68.3	963	266	10.13	13.2	714
15H-5, 145-150	138.1	7.57	4.30	34.8	49.66	12.11	573.0	26.80	78.2	1096	507	10.31	10.0	376
18X-4, 145-150	165.1	7.41	4.37	34.8	45.72	13.73	569.0	24.95	98.1	1080	705	9.78	8.8	632
21X-3, 145-150	192.1	7.49	4.20	34.5	41.30	15.11	567.0	23.12	112.7	1037	913	9.39	9.4	347
25X-4, 145-150	231.6	7.58	3.97	34.4	36.43	16.94	566.0	21.19	127.5	1092	1087	9.74	10.0	344
114-704B-														
27X-5, 145-150	249.6	7.57	4.16	34.4	35.68	17.46	569.0	20.55	137.6	1073	1076	8.73	9.4	251
30X-2, 145-150	273.6	7.54	4.23	34.4	33.20	18.98	569.0	19.21	158.1	1064	1151	8.33	8.8	475
33X-4, 145-150	305.1	7.48	4.70	34.1	29.93	20.26	563.0	18.57	179.6	1154	1132	8.68	8.1	407
36X-2, 145-150	330.6	7.41	4.38	34.0	28.77	21.11	575.0	18.35	182.5	1189	1132	8.77	8.8	437
39X-5, 145-150	363.6	7.41	4.34	34.0	27.27	21.97	565.0	17.25	178.9	1217	1219	8.51	11.3	492
42X-5, 97-107	391.7	7.29	4.53	34.0	25.68	22.76	565.0	17.31	161.9	1249	1271	8.47	14.4	464
46X-4, 140-150	428.6	7.36	3.37	34.0	25.06	22.59	566.0	17.19	131.1	1164	1166	7.98	18.8	748
48X-2, 140-150	444.6	7.35	3.23	34.0	24.26	23.31	566.0	16.35	123.0	1117	1273	7.72	23.2	910
52X-4, 140-150	478.1	7.36	3.90	34.1	22.84	24.25	567.0	15.71	113.6	1260	1302	7.90	21.9	508
54X-5, 140-150	498.6	7.41	3.43	34.0	23.37	24.02	566.0	16.66	108.3	1216	1280	7.50	23.2	474
58X-5, 140-150	536.6	7.46	3.35	34.1	23.28	24.33	563.0	16.63	98.9	1133	1301	7.63	26.3	
60X-5, 140-150	555.6	7.44	3.50	33.9	19.67	25.47	571.0	15.51	96.9	1139	1361	7.41	22.6	723
63X-4, 140-150	582.6	7.36	2.54	34.0	20.45	25.81	571.0	15.15	110.5	1134	1463	6.71	28.8	1178
70X-1, 140-150	644.6	7.42	2.89	33.9	15.91	27.13	566.0	13.48	124.5	1240	1535	7.37		
72X-2, 140-150	665.1	7.48	1.91	33.6	15.26	26.83	564.0	13.70	146.6	1247	1463	7.19		1341
^a Seawater		~7.76	2.38	(35.0)	54.05	10.68	558.6	28.90	69.3	~100	~90	10.45	~26.0	~100

Note: Values in parentheses are questionable and are not plotted in Figures 1-4.

^a Seawater concentrations are given for 35 per mil salinity, and the concentrations for nonconservative elements are for bottom water in the South Atlantic. Salinities were not measured at the drill sites, but typical deep and bottom water salinities in the South Atlantic are 34.6‰-34.9‰.

ACKNOWLEDGMENTS

We thank the co-chief scientists (Paul Ciesielski and Yngve Kristoffersen) for the opportunity for one of us (PNF) to participate on Leg 114. J. Bishop (Lamont) assisted with the barium analyses. Funding was provided by grants from the National Science Foundation (OCE-87-11588) and JOI/US-SACS (TAMRF-20116).

REFERENCES

- Baker, P. A., 1986. Pore-water chemistry of carbonate-rich sediments, Lord Howe Rise, southwest Pacific Ocean. In Kennett, J. P., von der Borch, C. C., et al., *Init. Repts. DSDP*, 90: Washington (U.S. Govt. Printing Office), 1249-1256.
- Baker, P. A., and Bloomer, S. H., 1988. The origin of celestite in deep-sea carbonate sediments. *Geochim. Cosmochim. Acta*, 52:335-339.
- Bishop, J., 1990. Determination of barium in seawater using vanadium/silicon modifier and direct-injection graphite furnace atomic absorption spectrometry. *Anal. Chem.*, 62:553-557.
- Froelich, P. N., Kim, K. K., Jahnke, R. J., Burnett, W. R., and Deakin, M., 1983. Pore water fluoride in Peru continental margin sediments: uptake from seawater. *Geochim. Cosmochim. Acta*, 47:1605-1612.
- Froelich, P. N., Mortlock, R. A., and Shemesh, A., 1989. Inorganic germanium and silica in the Indian Ocean: biological fractionation during (Ge/Si)_{opal} formation. *Global Biogeochem. Cycl.*, 3:79-88.
- Gieskes, J. M., 1974. Interstitial water studies, Leg 25. In Simpson, E. S. W., Schlich, R., et al., *Init. Repts. DSDP*, 25: Washington (U.S. Govt. Printing Office), 361-394.
- _____, 1981. Deep-sea drilling interstitial water studies: implications for chemical alteration of the oceanic crust, Layers I and II. In Warner, T. E., Douglas, R. C., and Winterer, E. L. (Eds.), *The Deep Sea Drilling Project: A Decade of Progress*. Spec. Publ. Soc. Econ. Paleontol. Mineral., 32:149-167.
- _____, 1983. The chemistry of interstitial waters of deep-sea sediments: interpretation of Deep-Sea Drilling data. In Riley, J. P., and Chester, R. (Eds.), *Chemical Oceanography* (vol. 8): London (Academic Press), 223-269.
- Gieskes, J. M., Johnston, K., and Boehm, M., 1984. Interstitial water studies, Leg 74. In Moore, T. C., Rabinowitz, P. D., et al., *Init. Repts. DSDP*, 74: Washington (U.S. Govt. Printing Office), 701-711.
- Gieskes, J. M., and Lawrence, J. R., 1981. Alteration of volcanic matter in deep-sea sediments: evidence from chemical composi-

- tion of interstitial waters from deep sea drilling cores. *Geochim. Cosmochim. Acta*, 45:1687-1703.
- Gieskes, J. M., and Peretsman, G., 1985. *Water Chemistry Procedures Aboard JOIDES Resolution - Some Comments*. ODP Tech. Note, 5.
- Manheim, F. T., and Sayles, F. L., 1974. Composition and origin of interstitial waters of marine sediments based on deep sea drill cores. In Goldberg, E. D. (Ed.), *The Sea* (vol. 5): New York (Wiley), 527-568.
- McDuff, R. E., 1981. Major cation gradients in DSDP interstitial waters: the role of diffusive exchange between seawater and upper oceanic crust. *Geochim. Cosmochim. Acta*, 45:1705-1713.
- _____, 1985. The chemistry of interstitial waters, Deep Sea Drilling Project Leg 86. In Heath, G. R., Burckle, L. H., et al., *Init. Repts. DSDP*, 86: Washington (U.S. Govt. Printing Office), 675-687.
- Mortlock, R. A., and Froelich, P. N., 1989. A simple method for the rapid determination of biogenic opal in pelagic marine sediments. *Deep-Sea Res., Part A*, 36:1415-1426.
- Shemesh, A., Mortlock, R. A., and Froelich, P. N., 1989. Late Cenozoic Ge/Si record of marine biogenic opal: implications for variations of riverine fluxes to the ocean. *Paleoceanography*, 4:221-234.
- Shipboard Scientific Party, 1988. Explanatory Notes. In Ciesielski, P. F., Kristoffersen, Y., et al., *Proc. ODP, Init. Repts.*, 114: College Station, TX (Ocean Drilling Program), 3-22.
- von Damm, K. L., 1983. Chemistry of submarine hydrothermal solutions at 21° North, East Pacific Rise and Guaymas Basin, Gulf of California [Ph.D. dissert.]. Woods Hole Oceanographic Inst./MIT, Woods Hole, MA.

Date of initial receipt: 4 April 1989

Date of acceptance: 12 November 1989

Ms 114B-153

SITE 699

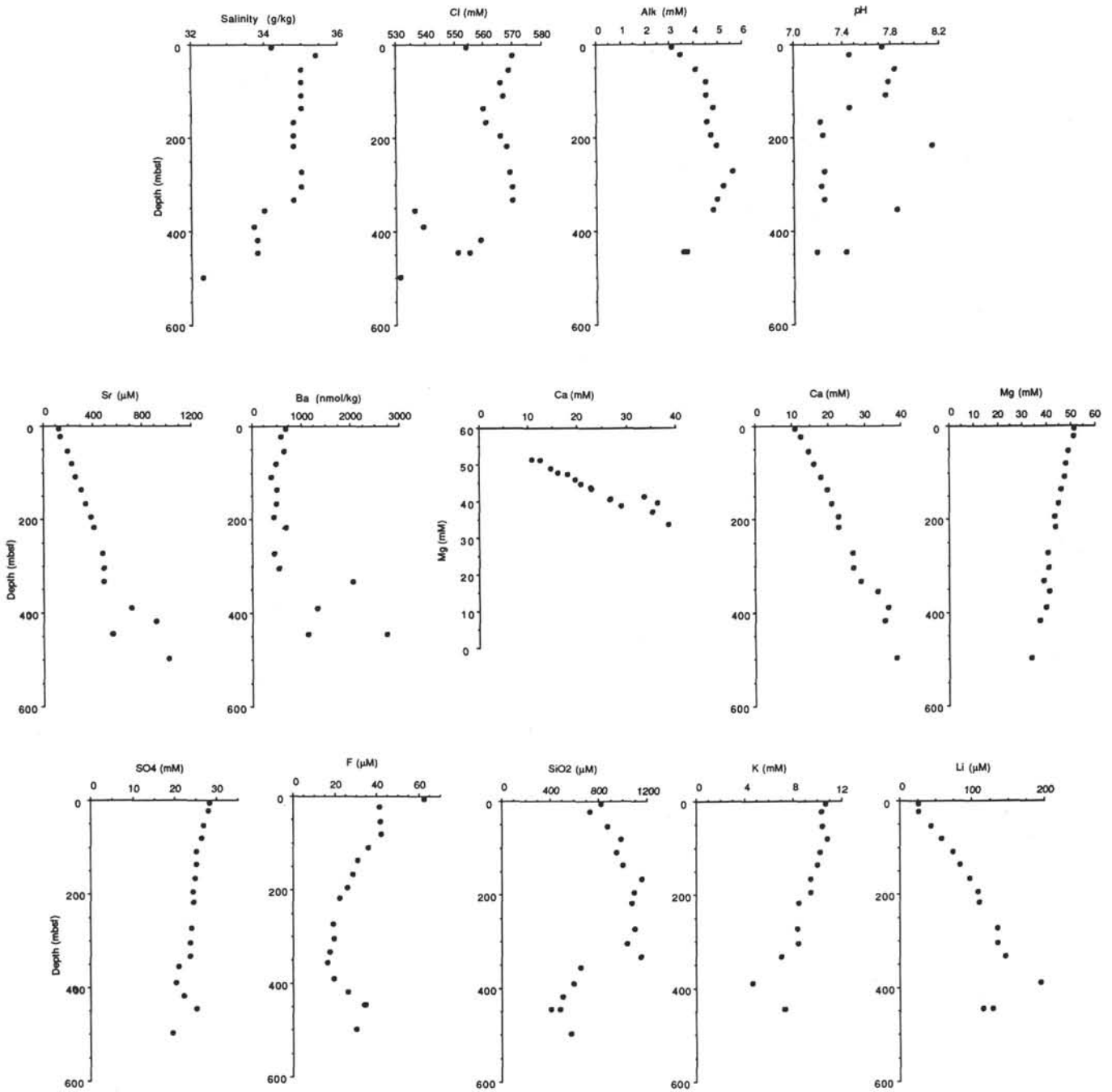


Figure 1. Vertical profiles of pore-water constituents vs. depth at Sites 699-702 and 704. The central plot is pore-water calcium vs. magnesium.

SITE 700

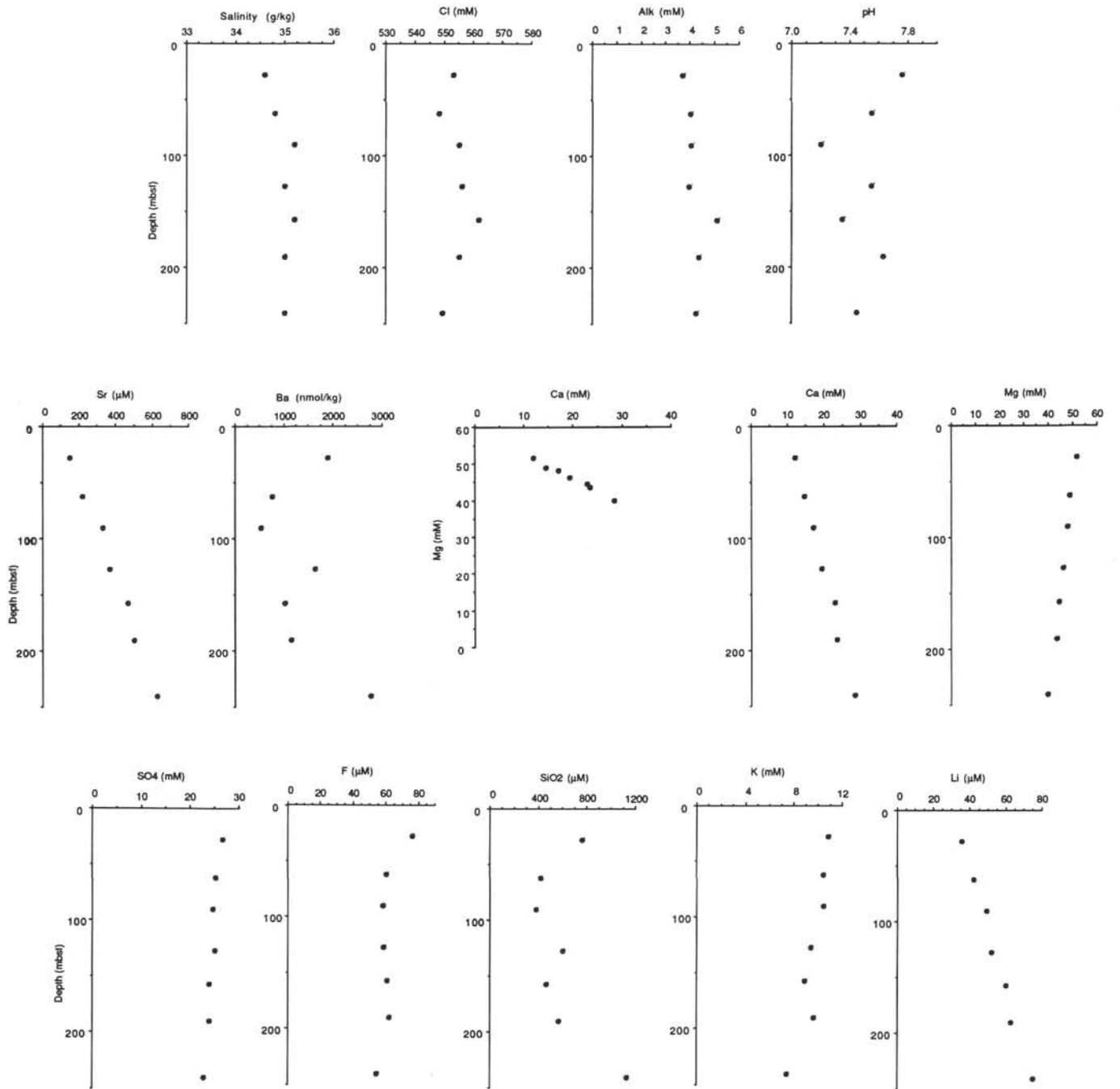


Figure 1 (continued).

SITE 701

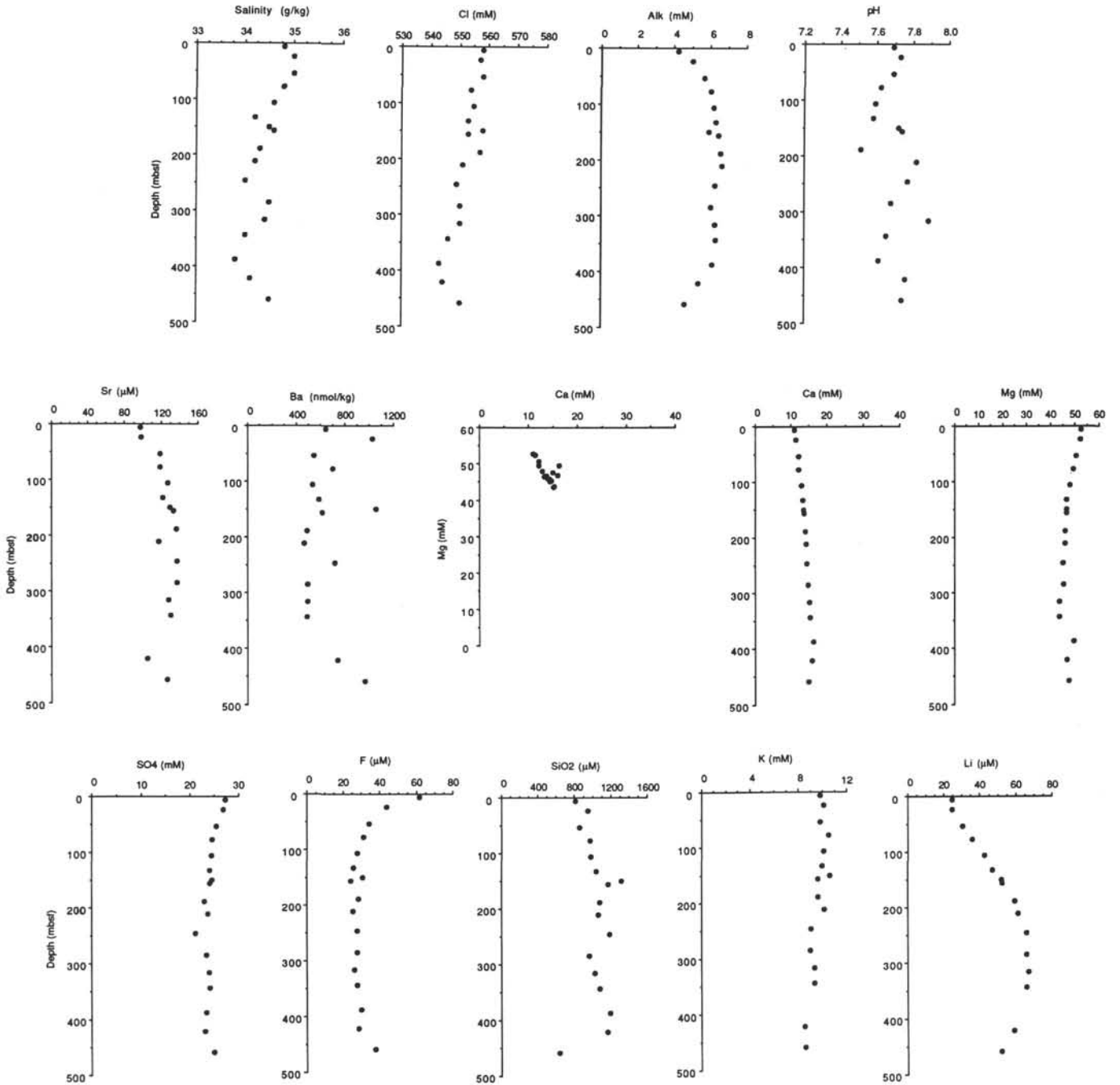


Figure 1 (continued).

SITE 702

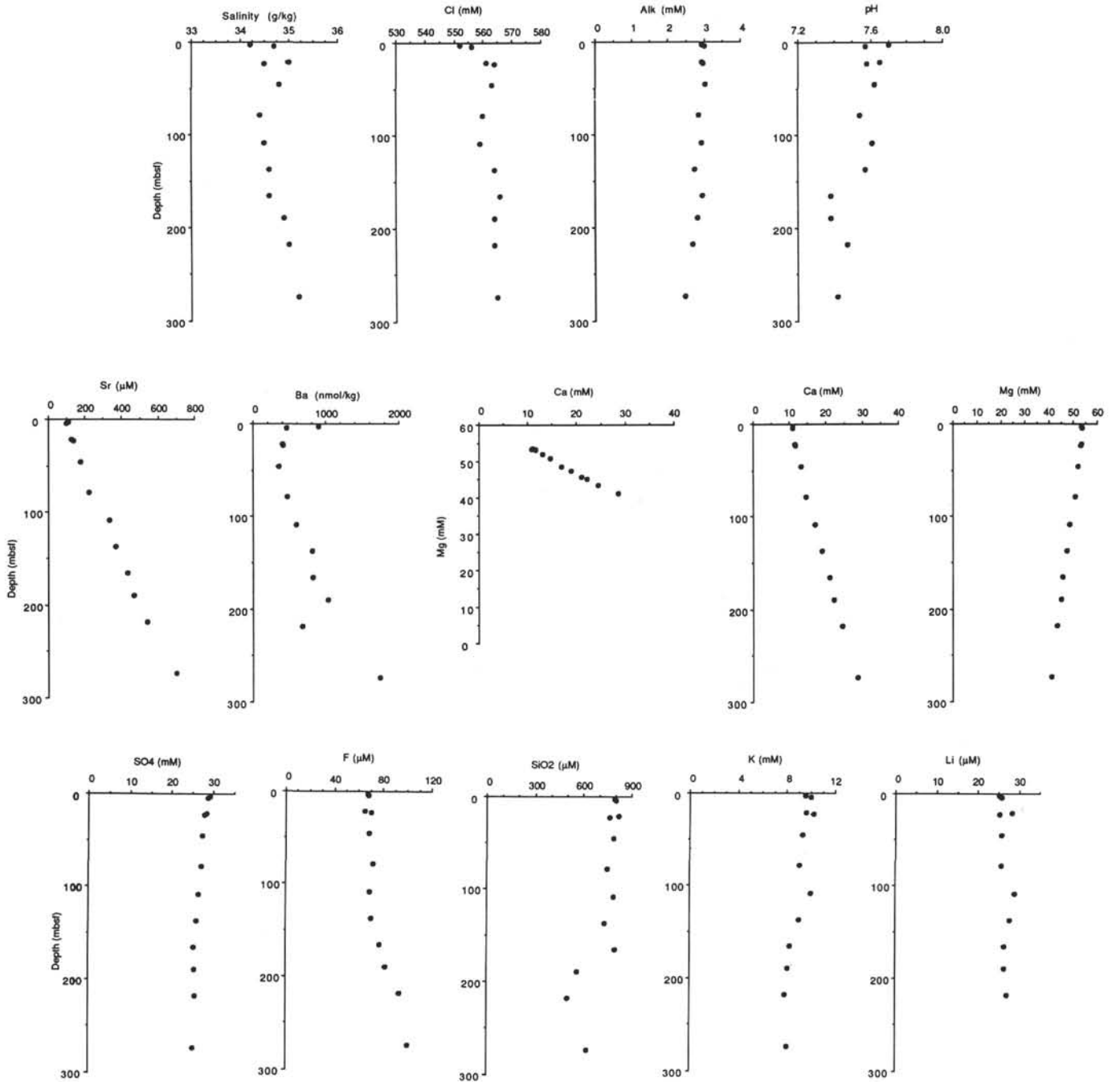


Figure 1 (continued).

SITE 704

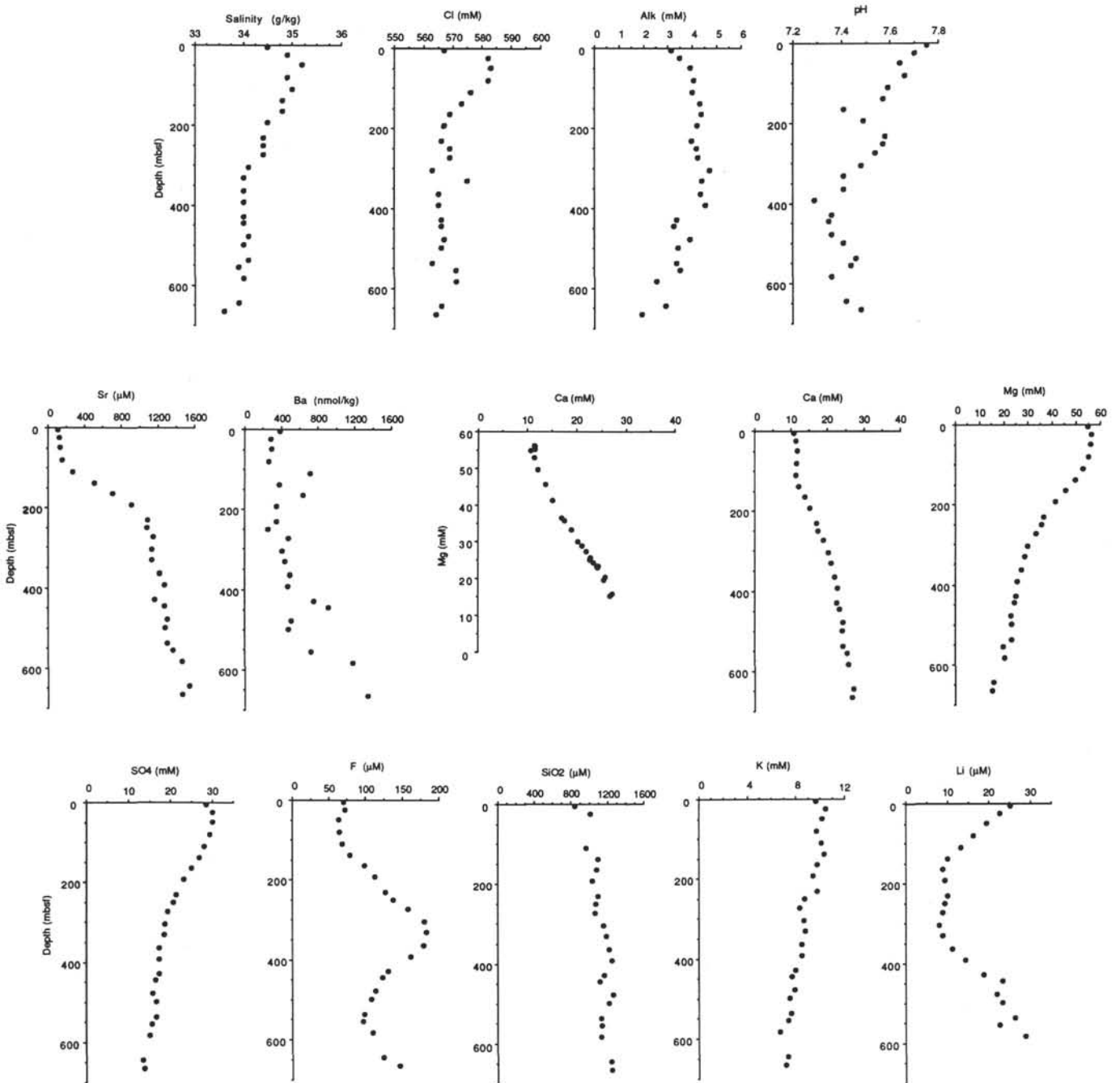


Figure 1 (continued).

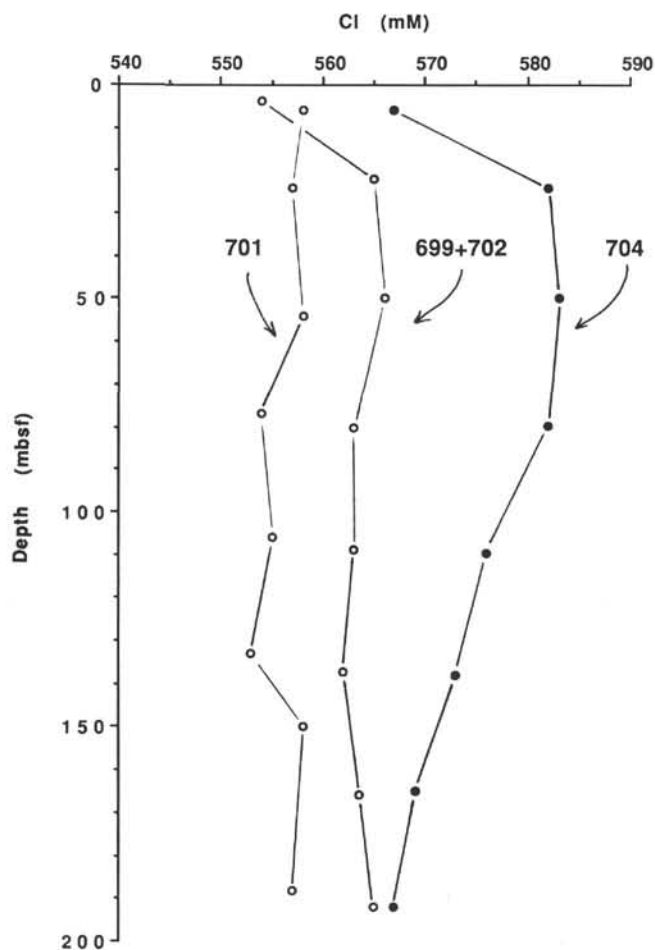


Figure 2. Pore-water chloride concentrations vs. depth. The data from Sites 699 and 702 were averaged for this plot. Site 701 is presently under the influence of AABW, while Sites 699, 702, and 704 are under CPDW and NADW. Except for Site 701, these profiles reflect the diffusion downward into the sediment column of Pleistocene variations in bottom-water chloride concentrations related both to whole-ocean salinity changes (glacial to interglacial continental ice volume changes) and to local water-mass variations (NADW).

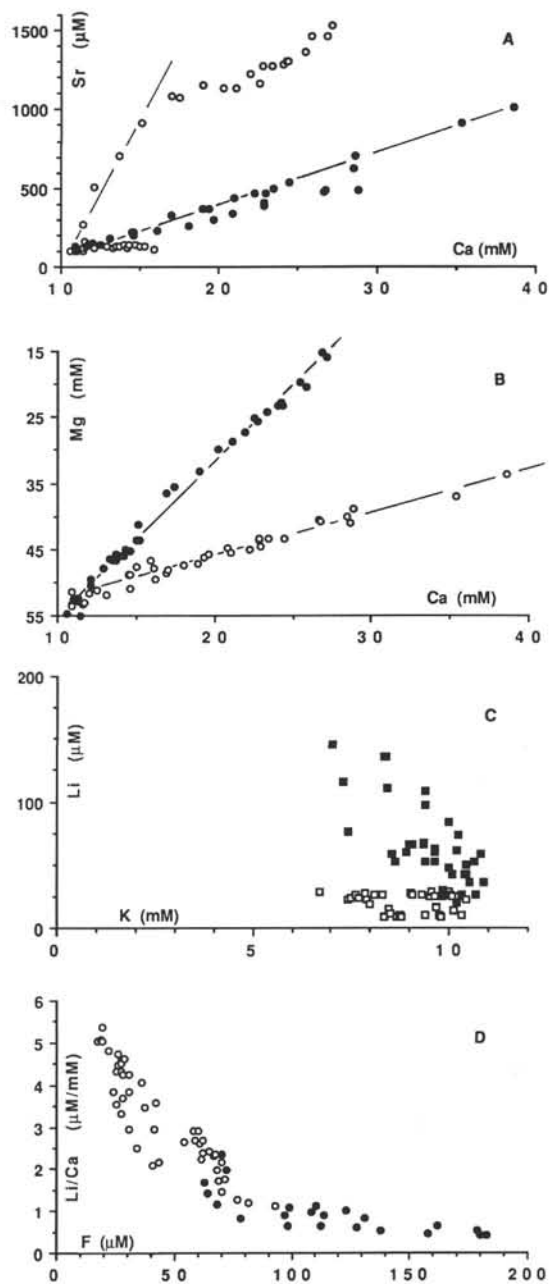


Figure 3. A. Pore-water strontium vs. calcium for all sites. Symbols for Sites 699, 700, and 702 are solid circles; Sites 704 (upper points) and 701 (lower points) are open circles. The straight line through the solid symbols has a slope (Sr/Ca) of 36×10^{-3} . The straight line through the open symbols has a slope of 220×10^{-3} . B. Pore-water magnesium vs. calcium for all sites. Symbols for Sites 699, 700, and 702 are open circles. The line through these points has a $\delta\text{Mg}/\delta\text{Ca}$ ratio of -0.5 , indicative of diffusive exchange with basement via low-temperature basalt-seawater reactions and conservative behavior in the sediment column (absence of ash and dolomitization). Symbols for Sites 701 and 704 are solid circles. The line through these points has a $\delta\text{Mg}/\delta\text{Ca}$ slope of -2.0 , indicative of diagenetic alteration of silicic volcanic ash contained in the sediment column at these sites. C. Pore-water lithium vs. potassium for all sites. Symbols for Sites 699, 700, and 701 are solid squares. Open squares are Sites 702 and 704. D. Pore-water Li/Ca ratios vs. F for all sites. Symbols for Site 704 are solid circles; all other sites are open circles.

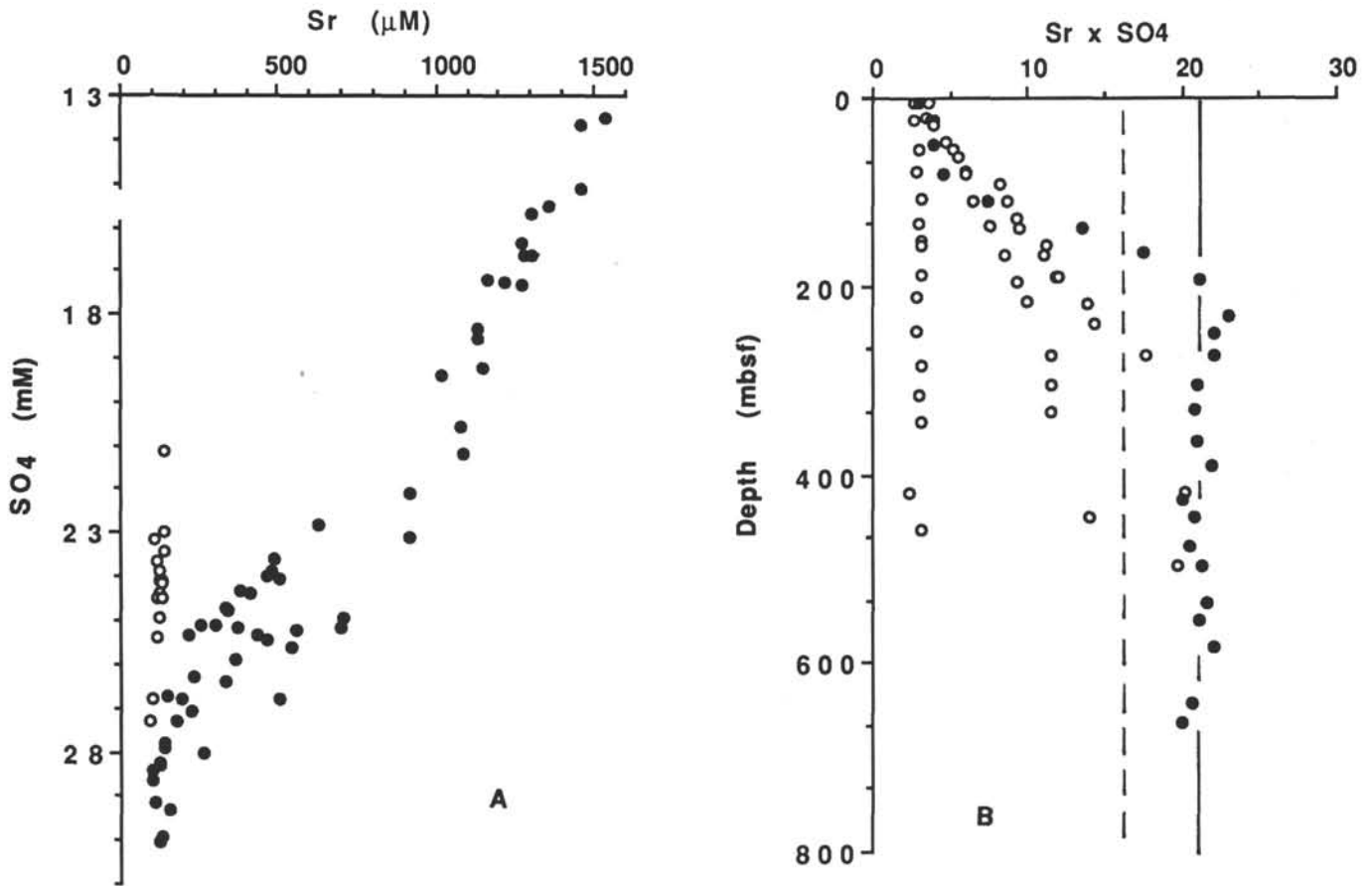


Figure 4. **A.** Pore-water strontium vs. sulfate concentrations. Symbols for Sites 699, 700, 702, and 704 are solid circles; the symbol for Site 701 is an open circle. **B.** The ICP for celestite ($\text{Sr} \times \text{SO}_4$) plotted vs. depth for all sites. Symbols for Sites 699–702 are open circles; the symbol for Site 704 is a solid circle. The vertical solid line represents an ICP = 21×10^{-6} , suggested as the solubility product for equilibrium with celestite at Site 704 (water depth = 2500 m). The vertical dashed line is for an ICP = 16×10^{-6} from sites on the Lord Howe Rise (water depth = 1000 m; Baker, 1986).